G9a/GLP targeting in MM promotes autophagy-associated apoptosis and boosts proteasome inhibitor–mediated cell death

Eva de Smedt, Julie Devin, Catharina Muylaert, Nicolas Robert, Guilhem Requirand, Philip Vlummens, Laure Vincent, Guillaume Cartron, Ken Maes, Jerome Moreaux, et al.

blood advances

American Society of Hematology
2021 L Street NW, Suite 900,
Washington, DC 20036
Phone: 202-776-0544 | Fax 202-776-0545
bloodadvances@hematology.org

G9a/GLP-targeting in MM promotes autophagy-associated apoptosis and boosts proteasome inhibitor mediated cell death

Tracking no: ADV-2020-003217R1

Elke De Bruyne (Vrije Universiteit Brussel, Belgium) Eva De Smedt (Vrije Universiteit Brussel, Belgium) Julie Devin (Institute of Human Genetics, France) Catharina Muylaert (Vrije Universiteit Brussel, Belgium) Nicolas Robert (CHU Montpellier, France) Guilhem Requirand (Institute of Human Genetics, France) Philip Vlummens (Ugent, Belgium) Laure Vincent (CHU Montpellier,) Guillaume Cartron (CHU Montpellier UMR5535, France) Ken Maes (Vrije Universiteit Brussel, Belgium) Jerome Moreaux (CHU Montpellier, France)

Abstract:
Multiple myeloma (MM) is a (epi)genetic highly heterogeneous plasma cell malignancy, which remains mostly incurable. Deregulated expression and/or genetic defects in epigenetic modifying enzymes contribute to high-risk disease and MM progression. Overexpression of the histone methyltransferase G9a was reported in several cancers, including MM, correlating with disease progression, metastasis and poor prognosis. However, the exact role of G9a and its interaction partner G9a-like protein (GLP) in MM biology and the underlying mechanisms of action remain poorly understood. Here, we report that high G9a mRNA levels are associated with a worse disease outcome both in newly diagnosed and relapsed MM patients. G9a/GLP-targeting using the specific G9a/GLP inhibitors BIX01294 and UNC0638 induces a G1-phase arrest and apoptosis in MM cell lines and reduces primary MM cell viability. Mechanistic studies revealed that G9a/GLP-targeting promotes autophagy-associated apoptosis by inactivating the mTOR/4EBP1 pathway and reducing c-MYC levels. Moreover, genes deregulated by G9a/GLP-targeting are associated with repressive histone marks. G9a/GLP-targeting sensitizes MM cells to the proteasome inhibitors (PIs) bortezomib and carfilzomib, by (further) reducing mTOR signaling and c-MYC levels and activating p-38 and SAPK/JNK signaling. Therapeutic treatment of 5TGM1 mice with BIX01294 delayed in vivo MM tumor growth and co-treatment with bortezomib resulted in a further reduction in tumor burden and a significant prolonged survival. In conclusion, we provide evidence that the histone methyltransferases G9a/GLP support MM cell growth and survival by blocking basal autophagy and sustaining high c-MYC levels and G9a/GLP-targeting represents a promising strategy to improve PI-based treatment in patients with high G9a/GLP levels.

Conflict of interest: No COI declared

COI notes:

Preprint server: No;

Author contributions and disclosures: Conception and design: EDS, JD, JM and EDB Development and methodology: EDS, JD, JM and EDB Acquisition of data: EDS, JD, CM, JM and EDB Analysis and interpretation of data: EDS, JD, CM, KM, PV, NR, GR, LV, GC, JM and EDB Writing, review, and/or revision of the manuscript: EDS, JD, KM, PV, JM and EDB Administrative, technical, or material support: EDS, JD, KM, PV, JM and EDB

Non-author contributions and disclosures: No;

Agreement to Share Publication-Related Data and Data Sharing Statement: Data may be requested from the corresponding authors at Elke.De.Bruyne@vub.be and jerome.moreaux@igh.cnrs.fr.

Clinical trial registration information (if any):

G9a/GLP-targeting in MM promotes autophagy-associated apoptosis and boosts proteasome inhibitor mediated cell death.

Eva De Smedt[(1*)], Julie Devin[(2*)], Catharina Muylaert[(1)], Nicolas Robert[(2,3)], Guilhem Requirand[(2,3)], Philip Vlummens[(1,4)], Laure Vincent[(5)], Guillaume Cartron[(5)], Ken Maes[(1)], Jerome Moreaux[(2,3,6°)] and Elke De Bruyne[(1°)]

[(1)] *Department of Hematology and Immunology-Myeloma Center Brussels, Vrije Universiteit Brussel, Brussels, Belgium*
[(2)] *IGH, CNRS, Univ Montpellier, France*
[(3)] *CHU Montpellier, Laboratory for Monitoring Innovative Therapies, Department of Biological Hematology, Montpellier, France*
[(4)] *Hematology, Department of Internal Medicine, Ghent University Hospital, Ghent, Belgium*
[(5)] *CHU Montpellier, Department of Clinical Hematology, Montpellier, France*
[(6)] *Institut Universitaire de France (IUF), 75000 Paris, France*

[(*)] *Equally contributing first authors.*
[(°)] *Equally contributing senior authors.*

Corresponding authors: Prof. Dr. Elke De Bruyne, Vrije Universiteit Brussel (VUB), Department of Hematology and Immunology-Myeloma Center Brussels, Laarbeeklaan 103, B-1090 Brussels, Belgium; e-mail: Elke.De.Bruyne@vub.be and **Prof. Dr. Jerome Moreaux**, Laboratory for Monitoring Innovative Therapies Department of Biological Hematology, Hôpital Saint-Eloi - CHRU de Montpellier, av. Augustin Fliche 80, 34295 Montpellier Cedex 5, France; e-mail: jerome.moreaux@igh.cnrs.fr.

Running title: Therapeutic potential of G9a/GLP-targeting in MM.

Keywords: Multiple myeloma (MM), G9a, GLP, histone methyltransferases, proteasome inhibitors

Abstract word count: 250

Text word count: 4646

Number of Figures: 7

Number of references: 59

Key Points

- G9a/GLP-targeting in MM induces autophagy-associated apoptosis by blocking mTOR/4EBP1 signaling and reducing c-MYC levels.
- G9a/GLP-targeting represents a promising strategy to improve proteasome inhibitor-based treatment in patients with high G9a/GLP levels.

Abstract

Multiple myeloma (MM) is a (epi)genetic highly heterogeneous plasma cell malignancy, which remains mostly incurable. Deregulated expression and/or genetic defects in epigenetic modifying enzymes contribute to high-risk disease and MM progression. Overexpression of the histone methyltransferase G9a was reported in several cancers, including MM, correlating with disease progression, metastasis and poor prognosis. However, the exact role of G9a and its interaction partner G9a-like protein (GLP) in MM biology and the underlying mechanisms of action remain poorly understood. Here, we report that high G9a mRNA levels are associated with a worse disease outcome both in newly diagnosed and relapsed MM patients. G9a/GLP-targeting using the specific G9a/GLP inhibitors BIX01294 and UNC0638 induces a G1-phase arrest and apoptosis in MM cell lines and reduces primary MM cell viability. Mechanistic studies revealed that G9a/GLP-targeting promotes autophagy-associated apoptosis by inactivating the mTOR/4EBP1 pathway and reducing c-MYC levels. Moreover, genes deregulated by G9a/GLP-targeting are associated with repressive histone marks. G9a/GLP-targeting sensitizes MM cells to the proteasome inhibitors (PIs) bortezomib and carfilzomib, by (further) reducing mTOR signaling and c-MYC levels and activating p-38 and SAPK/JNK signaling. Therapeutic treatment of 5TGM1 mice with BIX01294 delayed *in vivo* MM tumor growth and co-treatment with bortezomib resulted in a further reduction in tumor burden and a significant prolonged survival. In conclusion, we provide evidence that the histone methyltransferases G9a/GLP support MM cell growth and survival by blocking basal autophagy and sustaining high c-MYC levels and G9a/GLP-targeting represents a promising strategy to improve PI-based treatment in patients with high G9a/GLP levels.

1. Introduction

Multiple Myeloma (MM) is a highly heterogeneous malignancy characterized by the accumulation of monoclonal plasma cells in the bone marrow (BM).[1] MM comprises 10% of all hematological cancers, making it the second most common blood cancer after non-Hodgkin lymphoma.[2] Despite significant improvements in the treatment of MM, most patients still relapse due to the development of drug resistance. Defects in epigenetic processes such as DNA methylation, histone modifications and noncoding RNAs are well-known to contribute to MM pathogenesis. Given the indisputable role of these epigenetic defects in MM pathogenesis and their reversible nature, several approaches have been pursued to target the involved chromatin modifying enzymes.[3] The most clinically advanced epigenetic drug in MM is the histone deacetylase inhibitor (HDACi) panobinostat. This pan-HDACi was FDA/EMA approved in 2015 for the treatment of relapsed/refractory MM patients. However, panobinostat treatment comes with the cost of a high-risk for high grade toxicities, thus limiting its broad application. To circumvent this, efforts are now increasingly focusing on the role of specific histone methylation marks in MM pathogenesis.[3]

Arginine and lysine residues of the N-terminal tails of histone 3 and 4 are methylated or demethylated by histone methyltransferases (HTMs) and histone demethylases respectively, resulting in gene silencing or activation depending on the site of methylation and the number of methyl groups added.[3,4] The HTM G9a, also known as EHMT2, mediates mono- and dimethylation of histone 3 lysine 9 (H3K9me, H3K9me2). In general, H3K9me and H3K9me2 are associated with heterochromatin formation and gene silencing.[3,5] In addition, G9a acts as a scaffolding protein for other chromatin-associated molecules like heterochromatin protein 1, which in turn recruits DNA methyltransferase 1 (DNMT1) to the DNA, thus further enforcing transcriptional silencing.[3] Recently, G9a was also shown to facilitate MYC-mediated transcriptional repression by directly interacting with MYC through the MYC box II region.[6] An important interaction partner of G9a is the highly homologous G9a-like protein (GLP). Formation of this heterodimeric structure appears crucial for *in vivo* methyltransferase activity, since loss of either G9a or GLP reduces H3K9me/me2 levels.[3,7]

G9a is overexpressed in many different cancer types, including MM, resulting in the repression of tumor suppressor genes, like p53, CDH1, RUNX3 and E-cadherin.[3,8] High G9a expression is often associated with poor prognosis and G9a-targeting, using shRNA or specific small molecule inhibitors, inhibits proliferation, migration and metastasis of cancer cells.[3,4,9,10] A recent study showed that simultaneous targeting of DNMTs and G9a in acute

myeloid leukemia (AML), acute lymphoblastic leukemia (ALL) and diffuse large B-cell lymphoma (DLBCL) cell lines using the dual G9a/DNMTs inhibitor CM-272 inhibits proliferation and promotes apoptosis by inducing interferon-stimulated genes and immunogenic cell death.[11] Moreover, CM-272 significant prolonged survival of AML, ALL and DLBCL xenograft mice. The authors also suggested a potential role for G9a in MM as CM-272 decreased viability of human MM cell lines (HMCLs), but they did not determine the exact contribution of G9a in the CM-272-mediated MM cell death. In MM, copy number amplifications of G9a are frequent in patient samples.[12] Moreover, only very recently, G9a was shown overexpressed in HMCLs and G9a shRNA inhibited proliferation in vitro and tumorigenesis in xenograft mice.[8] However, the mechanisms of action were not thoroughly investigated nor was the capacity to boost the anti-myeloma activity of proteasome inhibitors. Moreover, to the best of our knowledge, no studies have yet investigated the expression and prognostic value of GLP in MM patients nor have they validated the therapeutic value of G9a/GLP-targeting using primary human MM samples and syngeneic, immunocompetent murine myeloma models.

Here, we investigated the expression and prognostic value of G9a and GLP in MM patients and the therapeutic potential of G9a/GLP-targeting using a large panel of cell lines, primary MM samples and the fully immunocompetent murine 5TGM1 model. In addition, we also explored the potential of G9a/GLP-targeting to boost the anti-myeloma activity of proteasome inhibitors (PIs).

2. Methods

2.1 Cell lines

The HMCLs AMO-1, OPM-2 and LP-1 were obtained from ATCC (Molsheim, France). These HMCLs and the murine MM cell lines 5T33MMvt and 5TGM1 were cultured in RPMI-1640 medium, supplemented with 10% FCS (Biochrom AG, Berlin, Germany) and 2mM L-glutamine. The IL-6 dependent cell lines XG-1, XG-2, XG-7, XG-11, XG-19, XG20 and XG-24 were obtained as previously described and maintained in the presence of 2ng/ml recombinant IL-6 (R&D systems, Oxon, UK), 10% FCS and 2mM L-glutamine.[13] Cell line identity was regularly checked by short-tandem repeat analysis and cells were regular screened for mycoplasma contamination.

2.2 Mice

C57Bl/KaLwRij mice were purchased from Envigo (Horst, The Netherlands). Mice were housed and treated following conditions approved by the Ethical Committee for Animal Experiments, VUB (CEP 14-281-5). The 5TGM1 model originated from aging C57BL/KaLwRij mice that spontaneously developed 5T33MM.[14] At day 0, naive C57BL/KaLwRij mice were injected with $2x10^6$ 5TGM1 cells containing firefly luciferase.[15] In a first experiment, mice were treated 3 times a week with 20mg/kg BIX01294 for 2 weeks via intraperitoneal injection in a therapeutic setting; with injections starting at the moment of established disease (day 14). Tumor development was monitored by non-invasive *in vivo* bioluminescence imaging (BLI) measuring total photon flux at day 30 using the Biospace Lab Photo Imager. D-luciferin (Promega Corporation, Madison, USA) was administrated intravenously. When individual mice showed signs of morbidity, they were sacrificed. In a second experiment, mice with established disease were treated with BIX01294 (10mg/kg, intraperitoneal injection, 3 times per week) and/or bortezomib (0.6mg/kg, subcutaneous injection, 2 times per week). When vehicle mice showed signs of morbidity, all mice were sacrificed and the effect on BM plasmacytosis was analyzed. BM mononuclear cells were isolated and spotted onto microscope slides using a cytocentrifuge. The slides were then stained by May-Grünwald-Giemsa for manual counting of the BM plasmacytosis. Finally, in a third experiment, mice with established were treated similar as in experiment 2, but this time the effect on overall survival was analyzed.

2.3 Gene expression data

The expression and prognostic value of G9a and GLP mRNA in terms of overall survival (OS) was determined using the publicly available RNAseq data of newly diagnosed MM patients from the Multiple Myeloma Research Foundation's (MMRF) CoMMpass study (https://research.themmrf.org/, release IA12). In addition, we also performed RNAseq analysis on BM samples collected from 68 patients treated with high-dose Melphalan and autologous stem cell transplantation. BM samples were collected after patients' written informed consent in accordance with the Declaration of Helsinki and institutional research board approval from Montpellier University Hospital. MM cells were purified using anti-CD138 MACS microbeads (Miltenyi Biotec, Bergisch Gladbach, Germany). We termed this validation cohort the Montpellier cohort. We also used Affymetrix data of relapsed MM patients subsequently treated with bortezomib (GSE9782) from the study of Mulligan et al.[16] To determine the effect of G9a/GLP-targeting on gene expression, OPM2, XG20 and XG24 cells were cultured for 24 hours with/without 5 μM BIX01294 or UNC0638. RNA samples were collected as previously described and their gene expression profile (GEP) obtained using Affymetrix U133 plus 2.0 microarrays.[17]

2.4 Statistical analysis

Statistical analysis was performed using GraphPad Prism 5.0 software and Genomicscape. A Mann-Whitney and one-way ANOVA test was used to compare 2 groups or multiple groups respectively. GEP data was normalized with MAS5 algorithm and analysed with GenomicScape and R and Bioconductor programs.[18,19] Gene set expression analysis (GSEA) was used to identify genes and pathways differentially expressed. Difference in overall survival was assayed with a log-rank test and survival curves plotted using the Kaplan-Meier method. The prognostic value of G9a and GLP was computed using maximally selected rank test from R package Maxstat, allowing to determine the optimal cut point for continuous variables.[20]

2.5 Data sharing statement

Data may be requested from the corresponding authors at Elke.De.Bruyne@vub.be and jerome.moreaux@igh.cnrs.fr.

For further details and other methods, see supplemental methods.

3. Results

3.1 High G9a levels are associated with a worse outcome in MM patients

First we evaluated the G9a and GLP mRNA levels in newly diagnosed patients using the publicly available RNAseq data of 674 patients from the MMRF CoMMpass study. Both G9a and GLP were found heterogeneously expressed (Figure 1A). Next, we analyzed the relation between G9a and GLP mRNA levels and disease outcome using the Maxstat R algorithm.[21] Patients with high G9a mRNA levels had a significant worse outcome than patients with low G9a mRNA levels (Figure 1B). These findings were validated in a second, independent cohort of newly diagnosed patients (the Montpellier cohort, n=68) and in a cohort of 188 patients treated with bortezomib monotherapy after relapse (Figure 1C-D). In contrast, no significant association between GLP expression and outcome was identified in the different cohorts (Supplementary Figure S1). Together, these findings demonstrate that G9a is an adverse prognostic factor in MM and high G9a expression is associated with MM disease progression.

3.2 G9a/GLP-targeting impairs growth and survival of MM cells

To investigate the role of G9a/GLP in MM, we first assessed the effect of the small-molecule G9a/GLP inhibitors BIX01294 and UNC0638 on MM cell viability using a panel of 10 HMCLs. G9a/GLP-targeting resulted in a clear decrease in MM cell viability in most cell lines, with IC50 values ranging between 1,2-3,39 µM and 2,71-17,4 µM for BIX01294 and UNC0638 respectively (Figure 2A). Subsequent flow cytometric analysis revealed a significant drop in the number of cells in S-phase together with a clear accumulation of cells in the G0/G1-phase in OPM-2 and XG-20 cells, when cells were treated with 5 µM of either inhibitor (Figure 2B and Supplementary Figure S2). Treatment with BIX01294 also significantly increased the percentage Ki67 negative cells associated with quiescence and the number of apoptotic cells (Figure 2C-D). Finally, BIX01294 treatment reduced viability of primary human CD138+ MM cells in most patient samples tested (n=12, Figure 2E). Patient characteristics are provided in Supplementary Table S1.

To validate the role of G9a in the anti-myeloma effects mediated by BIX01294/UNC0638, we then performed loss of functions studies. XG-7 cells were transduced with doxycycline inducible lentiviral constructs expressing 3 different shRNAs targeting G9a (ShG9a#1-3). All three ShG9a constructs strongly reduced G9a mRNA and protein levels when doxycycline was added compared to control (Figure 3A-B). Moreover, genetic depletion of G9a by ShG9a construct 1 (shG9a#1) strongly reduced MM cell growth (Figure 3C).

3.3 G9a/GLP-targeting induces autophagy-associated apoptosis in MM cells

Next, we investigated the molecular mechanisms underlying the anti-myeloma activity of G9a/GLP inhibition. To confirm the on-target effects of BIX01924, we first evaluated the effect on H3K9 methylation levels. BIX01294 strongly reduced H3K9me2 and/or H3K9me3 levels (the latter only in OPM-2 cells) while leaving H3K9me levels largely unaffected, thus confirming effective inhibition of G9a/GLP enzymatic activity under these treatments (Figure 4A). In addition, genetic inhibition of G9a (ShG9a#1-3) resulted in a similar decrease in H3K9me2 and H3K9me3 levels (Figure 4B).

Since many reports have shown a clear role for G9a in negatively regulating autophagy, we next performed immunofluorescent staining for LC3B-II and α-tubulin.[26,27] As expected, we observed a clear increase in LC3B-II puncta in MM cells upon treatment with either BIX01294 or UNC0638 (Figure 4C and Supplementary Figure S3). This increase in LC3B-II was also confirmed by western blot (Figure 4D-E). Western blot analysis further showed that BIX01294 blocks mTORC1-mediated autophagy inhibition and mTORC1-mediated protein translation as evidenced by decreased phosphorylation of Akt at serine residue (Ser) 473, ULK at Ser 757, mTOR at Ser2448, 4EBP1 at Thr37/46 and eIF4E at Ser209. BIX01294 treatment also strongly reduced Beclin and c-MYC levels, while increasing p21 levels (Figure 4D-E). Importantly, although BIX01294 also moderately increased the amount of active caspase3/7, addition of the pan-caspase inhibitor Q-VD-OPh did not rescue the cells from BIX01294 or UNC0638 mediated cell death as compared to melphalan-induced cell death, suggesting that the observed apoptosis is not caspase dependent (Supplementary Figure S4). In line with the western blot data, qRT-PCR also revealed a strong reduction of c-myc mRNA levels and deregulation of genes involved in autophagy regulation, including downregulation of mTOR and eIF4E and upregulation of ATG4 (Figure 4F and Supplementary Figure S5). Finally, we found that the well-known autophagy inhibitor 3-methyladenine (3-ME)[22] partially protected MM cells against BIX01294 mediated apoptosis, thus further confirming the role of autophagy induction in the BIX01294/UNC0638 mediated cell death (Figure 4G).

3.4 Genes deregulated by G9a/GLP-targeting are associated with repressive marks

To analyze transcriptional programs regulated by G9a/GLP in MM cells, OPM-2, XG-20 and XG-24 cells were treated with BIX01294 or UNC0638 for 24h and the GEP was analyzed using Affymetrix microarrays. Ninety-one genes were significantly upregulated and 23 downregulated in the treated cells compared to control (Fold change ≥ 1.5, FDR ≤ 0.05, Supplementary Table S2 and Supplementary Figure S6). GSEA analysis revealed a significant

enrichment in polycomb PRC2 target genes, genes associated with DNA methylation, HDAC targets and genes involved in immune response, interferon and chemokine pathways (Figure 5A). Among the upregulated genes, we validated the increased expression upon BIX-01294 treatment for CCL3, an important chemokine implicated in both immune surveillance and tolerance[23], using qRT-PCR (Figure 5B). Importantly, 73 of the upregulated genes were found associated with the H3K9me3 mark (Figure 5C, Supplementary Table S3). Apart from CCL3, we also identified EGR2, described as a tumor suppressor gene in MM, TRIM69 involved in autophagy, CASP1 taking part in the activation of pyroptosis and inflammasome, and UBE2QL1 involved in ubiquitination and degradation of mTOR (Supplementary Figure S7).[24-27]

3.5 BIX01294 delays tumor progression in vivo

Next, we wanted to validate the anti-myeloma activity of G9a/GLP-trageting *in vivo* using the syngeneic, immunocompetent murine 5TMM models. For this, we first confirmed the anti-myeloma activity *in vitro* using the murine cell lines 5T33MMvt and 5TGM1 and primary murine 5T33MMvv cells. Again, BIX01294 and UNC0638 potently reduced MM cell viability and induced apoptosis (Figure 6A-B). Since BIX01294 is known to have a narrow therapeutic window[28], we then first evaluated the effect of two weeks of BIX01294 treatment (10 and 20 mg/kg) on white blood cell, red blood cell and platelet count and hemoglobin levels in naïve mice. We observed no major changes in these hematological parameters upon treatment with BIX01294 (Supplementary Figure S8). Next, we studied the *in vivo* effect of BIX01294 treatment in the 5TGM1 model. Mice with established disease were treated therapeutically with BIX01294 (20 mg/kg) for 2 weeks (Figure 6C). Tumor development was monitored on day 30 post-inoculation by non-invasive *in vivo* BLI. BIX01294 treatment strongly reduced tumor burden compared to vehicle treated mice (Figure 6D). Moreover, BIX01294 monotherapy significantly prolonged overall survival of 5TGM1 inoculated mice compared to vehicle (Figure 6E).

3.6 G9a/GLP-targeting potentiates the anti-MM effect of proteasome inhibitors

We also investigated if BIX01294 could increase the therapeutic benefit of the PIs bortezomib and carfilzomib. Co-treatment of MM cells with bortezomib and BIX01294 strongly increased the number of apoptotic cells compared to both single agents in murine cell lines, but not in the HMCL (Supplementary Figure S9). Nevertheless, combination experiments using the second-generation PI carfilzomib did significantly and synergistically increase the percentage of apoptotic cells compared to single agent therapy and this both in murine cells

and HMCL (Figure 7A and Supplementary Figure S9). Importantly, the combinatory effect was also confirmed when targeting G9a via genetic depletion using shG9a#1 in the XG-7 cells (IC50 of 0.0261 nM for DOX compared to 0.358 for control, Figure 7B) and on primary MM cells (Figure 7C, patient characteristics provided in Supplementary Table 4). In contrast, we observed only minimal (combinatory) effects of BIX01297 and/or carfilzomib on the non-myeloma fraction of the primary BM samples (Supplementary Figure S8). Moreover, shG9a#1 did not sensitize the XG-7 cells to the immunomodulating agent lenalidomide and only minimal to pomalidomide (Supplementary Figure S9). Western blot analysis revealed that the increased sensitivity toward PIs was associated with a further reduction in mTOR signaling and c-MYC levels, and an increase in p-38 and SAPK/JNK signaling (Figure 7D). In a proof of principle study, we then investigated the combination of BIX01294 and bortezomib *in vivo*. In a first experiment, 5TGM1 mice with established disease were treated with a suboptimal dose of bortezomib and/or BIX01294 in a therapeutic setting (Figure 7E) and the effect on tumor burden was evaluated. We observed a significant reduction in the BM plasmacytosis in mice treated with bortezomib ($p<0.05$) and the combination ($p<0.001$) compared to vehicle treated mice. Moreover, although not significant, we observed a clear trend for a further reduction in tumor burden in combo treated mice versus bortezomib treated mice (Figure 7E). Of note, we observed no significant weight loss upon 2 weeks of treatment with BIX1294 and/or carfilzomib (Supplementary Figure S8). Finally, in a second experiment, we also evaluated the effect on overall survival. In line with the effects on tumor burden, a suboptimal dose of BIX01294 did not change the overall survival of 5TGM1-inoculated mice (Figure 7F). In contrast, and as expected, bortezomib did significantly prolong overall survival of the 5TGM1 mice, with a median survival of 41 days compared to 35 days for the vehicle treated mice. Importantly, combining bortezomib with BIX01294 further prolonged overall survival of the mice compared to treatment with either agent alone (median survival of 48 days, $p<0.05$), thus again confirming that BIX01294 boosts the anti-myeloma activity of PIs.

4. Discussion

Aberrant epigenetic regulation plays a major role in cancer, including MM. The reversible nature of the epigenetic modifications has led to the development of many drugs targeting the epigenetic machinery. The classical, broad-acting DNMT inhibitors and HDACi have proven useful in MM therapy, especially the pan-HDACi panobinostat. However, these epidrugs are often associated with severe toxicity issues, thus limiting the broad application in the clinic. Therefore, novel drugs targeting methylation of specific histone lysine residues are currently under investigation.[3] Previous studies have shown increased expression of the HMT G9a in different cancers, associated with tumor suppressor silencing, migration and a worse outcome.[3] Also in MM, G9a overexpression in HMCLs was recently reported and patients with high G9a levels were found to display a significant worse outcome.[8] In the present study, we validated the prognostic value of G9a in two independent cohorts of newly diagnosed patients and one cohort of relapsed patients.

Given the important role of G9a in cancer, a growing number of G9a/GLP inhibitors have been developed and tested in the preclinical setting.[28] These inhibitors can be divided in substrate competitive inhibitors, S-adenosyl-methionine (SAM) cofactor competitive inhibitors and inhibitors with unclear mechanisms. Substrate competitive inhibitors specifically block the substrate binding site instead of competing with SAM and are thus more selective than the SAM competitive inhibitors. In our study, we used the substrate competitive inhibitors BIX01294 and UNC0638, with UNC0638 being an improved version of BIX01294 displaying superior selectivity for G9a and GLP and a superior toxicity/function ratio.[28] Both inhibitors were extensively reported to induce potent anti-tumor activity in various cancers.[3,28] In line with these studies, we found that BIX01294 and UNC0638 strongly reduced MM cell viability and growth and promoted apoptosis in human and murine MM cell lines. Importantly, in line with the earlier study reported by Zhang et al, genetic depletion of G9a using ShG9a also strongly reduced MM cell growth, thus confirming that the anti-myeloma effects induced by BIX01294/UNC0638 are at least partially mediated by G9a.[8] The potent anti-MM activity was also confirmed using primary patient samples and the syngeneic, fully immunocompetent murine 5TGM1 model. Only very recently, Zhang et al showed that G9a shRNA impairs RelB-dependent cell survival and proliferation of HMCLs and reduces MM growth in a xenograft model in a prophylactic setting.[8] Here, we show that simultaneous targeting of G9a/GLP for only 2 weeks in fully immunocompetent mice with established

disease (a therapeutic and thus more clinically relevant setting) also resulted in a significant delay in tumor progression.

G9a and GLP contribute to tumorigenesis via diverse molecular mechanisms.[3,4,28] The best-described mechanism is H3K9me2-mediated transcriptional repression of tumor suppressors.[3,4,28] Here, we show that G9a/GLP-targeting (using either chemical or genetic inhibition) resulted in a strong decrease in H3K9me2 levels. This is in line with reports showing that G9a/GLP complexes mainly catalyze H3K9me2.[7,8,28] Genes transcriptional affected by BIX01294 or UNC0638 in MM cells were significantly enriched in polycomb PRC2 target genes, genes associated with DNA methylation, HDAC targets and genes involved in immune response, interferon and chemokine pathways. These data underline that G9a/GLP target genes could comprise key MM tumor suppressors silenced through different epigenetic mechanisms, such as CASP1 and EGR2.[25,27]

A second well-described mechanism by which G9a contributes to cancer biology is through autophagy repression.[29-31] Autophagy is a highly regulated catabolic process stimulated via different stress stimuli.[32,33] Upon stimulation, cellular components are incorporated into autophagosomal vesicles, followed by fusion with lysosomes, forming autolysosomes and causing the degradation of the cellular content. The role of autophagy in cancer is still controversial, since it appears to prevent early tumor formation but is also able to promote tumor survival.[32-34] Under normal physiological conditions, autophagy plays an important role in maintaining cellular homeostasis. However, long-term and intensive autophagy can lead to caspase-independent cell death, called autophagy-associated apoptosis.[32-34] A common way to analyze autophagy is by studying the accumulation and intracellular localization of microtubule-associated protein light chain (LC3)-II. Previously, G9a/GLP-targeting using BIX01294 was shown to induce autophagy-associated apoptosis in different cancers.[30,31,35-37] In line with these reports, we found that both BIX01294 and UNC0638 promoted autophagy-associated apoptosis in MM cells, as evidenced by a strong increase in LC3B-II levels and LC3B puncta formation together with a strong increase in caspase-independent apoptosis. Furthermore, the autophagy inhibitor 3-methyladenine partially protected against BIX01294-induced apoptosis, thus further confirming the role of autophagy in the BIX01294-induced apoptosis.

The induction of autophagy is regulated via several signaling pathways, the most important being the mTOR-signaling pathway.[32,33] The serine/threonine kinase mammalian target of rapamycin (mTOR kinase) forms the catalytic subunit of two functionally distinct

multiprotein complexes, mTORC1 and mTORC2. The mTORC1-signaling pathway plays an important role in maintaining cellular homeostasis by promoting growth, survival, translation, ribosome biogenesis and lipid synthesis.[32,33] Aberrant activation of this pathway correlates with disease progression and resistance to therapy in MM.[38] Importantly, mTOR signaling inhibits autophagy both directly and indirectly.[32,33,39] Under physiological conditions, mTORC1 stimulates protein translation, cell growth and survival and inhibits autophagy by phosphorylating ULK1/2 at S757 and S637 residues, blocking its catalytic activity and interaction with AMPK. Upon autophagy induction, mTOR is inactivated allowing ULK1 S757/637 dephosphorylation. As a result, ULK1 will become activated and autophagosome membrane formation is started. In our study, we observed a clear decrease in phosphorylation of Akt, mTOR and ULK1 S757/637 in the MM cells upon BIX-01294 treatment. These findings are in line with previous reports showing that G9a targeting induces autophagy through the mTOR signaling pathway in cancer cells.[36,37] Moreover, G9a is also responsible for the epigenetic silencing of autophagy-related genes such as LC3B, WIPI1 and DOR in pancreatic cancer cells.[29] In line with this, we found that BIX01294/UNC0638 deregulated the expression of several autophagy related genes, including mTOR, WIPI1, ATG4D and ATG7, in MM cells. Furthermore, BIX01294 induces upregulation of UB2QL1, which is known to participate in mTOR ubiquitination and degradation.[26]

Importantly, we also observed a clear decrease in the phosphorylation and expression levels of the mTORC1 target 4EBP1 upon BIX01294 treatment. Previous studies have shown that 4EBP1 is inhibiting autophagy.[32] Importantly, hypophosophorylated 4EBPs will also block cap-dependent translation by binding with high affinity to eIF4E.[32,33] A key MM tumor suppressor likely to be strongly affected by blocking protein synthesis is the transcription factor c-MYC; a very unstable protein with an half-life of only 20 to 30 minutes.[40] C-MYC binds to promotor regions of genes involved in cell cycle regulation and metabolism.[41] Overexpression of c-MYC was reported in various cancers, including MM, where deregulated MYC expression is found in 50% of the patients.[42] An increase in c-MYC protein levels has been associated with MM onset and progression and an inferior overall survival.[38,42,43] In hematological cancers, c-MYC overexpression results in mTOR-mediated 4EBP1 hyperphosphorylation, thus creating a viscous cycle. Consequently, mTOR inhibition strongly decreases tumor burden *in vivo* in MM.[40] Other studies also demonstrated the importance of targeting the mTOR-cMYC axis in different cancers.[44,45] As expected, we observed a strong decrease in c-MYC protein levels upon BIX01294 treatment, indicating that G9a/GLP

inhibition also induces autophagy-associated apoptosis by targeting the mTORC1/4EBP1/c-MYC pathway in MM cells. Of note, epigenetic proteins have emerged as critical regulators of c-MYC at multiple levels in cancer.[46] In MM, targeting the bromodomain and extraterminal (BET) family member BRD4 using the BETi JQ-1 is well-known to potently suppress MYC transcription.[47-49] Moreover, we and others previously showed that treatment with HDACi and/or DNMTi suppresses MYC transcription and/or the MYC transcriptome.[47,50] In addition, we also showed that HDACi and/or DNMTi treatment down-regulates IRF4, an essential MM survival factor that also targets MYC.[51] In line with these reports, we found that G9a/GLP-targeting also suppresses MYC transcription. Of interest, it was recently also shown in breast cancer that G9a interacts with MYC to drive tumorigenesis.[6] G9a appeared essential for MYC-mediated transcriptional repression and inhibiting G9a de-repressed expression of MYC-repressed genes resulting in suppressed MYC-driven tumor growth. Moreover, in line with our findings, the authors also observed a modest reduction in c-MYC protein levels upon G9a and/or GLP silencing when cells are cultured under normal growing conditions. Also, in human pancreatic ductal adenocarcinoma KP-4 cells it was moreover recently shown that BRD4 and G9a are working together to negatively regulate autophagy at the transcriptional level in growing conditions.[52] Targeting either BRD4 or G9a both enhanced autophagic flux, whereas simultaneous targeting of BRD4 and G9a did not further enhance autophagy activity, suggesting that they both act on the same pathway. Based on this, it is tempting to speculate that G9a and BRD4 are also working together to regulate the MYC transcriptome in MM. It will be interesting to investigate this further in future studies. Finally, similar to what we observed, the bivalent BETi AZD5153 was shown to repress MYC, E2F and mTOR target gene transcription in MM cells.[53] Moreover, the authors provided evidence that MM cell lines sensitive to AZD5153 exhibited a marked decrease in the level of mTOR pathway–associated proteins (including p-p70S6K, PRAS40 and p-4EBP1) following AZD5153 treatment, whereas MYC proteins levels were decreased in both sensitive and resistant cell lines, suggesting that MYC downregulation alone was not sufficient to modulate cell survival. Together with our findings, these reports indicate that G9a is positively regulating c-MYC expression in MM cells and G9a/GLP-targeting represents a compelling strategy to disrupt the mTORC1/4EBP1/c-MYC axis in MM.

Finally, a bidirectional interplay between the mTOR pathway and the ubiquitin proteasome system has been reported.[39] Blocking the proteasome results in the accumulation of proteins

and a decrease in the pool of amino acids available for protein synthesis, thus reducing mTOR signaling and stimulating autophagy.[38] PI-based treatments are one of the cornerstones of MM therapy. The PI bortezomib is used in the first line setting, while the second-generation inhibitor carfilzomib has been approved for relapsed/refractory MM patients. Both inhibitors bind to the catalytic site of the 20S proteasome, inducing growth arrest and cell death.[39,54] Studies in MM showed synergistic effects when combining mTOR inhibitors and bortezomib.[39,55] In addition, recent studies showed that inhibition of c-MYC also sensitizes MM cells to PI therapy.[38,56,57] In concordance, we found that BIX01294 sensitized MM cells to bortezomib and carfilzomib and this both *in vitro* and *in vivo*. The increased sensitivity towards PIs was associated with a further reduction in mTOR signaling and c-MYC levels and an increase in p-38 and JNK/c-Jun signaling. Zhao et al previously showed that autophagic cell death in non-small cell lung cancer is mediated through activation of the JNK and p38 MAPK pathways and inhibition of the mTOR signaling pathway.[58] In MM patients, low c-Jun levels are correlated with an inferior survival and bortezomib resistance and overexpression of c-Jun overcomes this resistance.[59] Thus, activation of the JNK/c-Jun pathway upon combination treatment could also explain the observed boosting effects.

Together, our data provide evidence that G9a/GLP-targeting in MM cells induces autophagy-associated apoptosis and sensitizes MM cells to PI-based therapy by inhibiting mTOR signaling and decreasing c-MYC levels. G9a/GLP-targeting thus represents a promising new strategy to improve PI-based therapy in $G9a^{high}$ myeloma patients.

5. Acknowledgments

This work was supported by grants form the international Myeloma Foundation (IMF), KomOpTegenKanker (KOTK), Fonds voor Wetenschappelijk Onderzoek (FWO), INCa (Institut National du Cancer) PLBIO18-362 PIT-MM and PLBIO19-098 INCA_13832FATidique, ANR (the French National Research Agency) under the "Investissements d'avenir" program with the reference ANR-16-IDEX-0006, ANR (TIE-Skip; 2017-CE15-0024-01), ANR-18-CE15-0010-01 PLASMADIFF-3D, SIRIC Montpellier Cancer (INCa_Inserm_DGOS_12553), Labex EpiGenMed and Institut Universitaire de France. We thank Carine Seynaeve, Lotte Jacobs and Charlotte Van De Walle for their expert technical assistance. We thank the MMRF for sharing the RNA sequencing and clinical data of the patients enrolled in the CoMMpass study through the MMRF genomics portal.

6. Authorship contributions

Conception and design: EDS, JD, JM and EDB

Development and methodology: EDS, JD, JM and EDB

Acquisition of data: EDS, JD, CM, JM and EDB

Analysis and interpretation of data: EDS, JD, CM, KM, PV, NR, GR, LV, GC, JM and EDB

Writing, review, and/or revision of the manuscript: EDS, JD, KM, PV, JM and EDB

Administrative, technical, or material support: EDS, JD, KM, PV, JM and EDB

7. Disclosure of conflict of interest

The authors have no conflicts of interest to declare.

8. References

1. Chesi M, Bergsagel PL. Advances in the pathogenesis and diagnosis of multiple myeloma. *Int J Lab Hematol.* 2015;37 Suppl 1:108-114.
2. Kyle RA, Durie BG, Rajkumar SV, et al. Monoclonal gammopathy of undetermined significance (MGUS) and smoldering (asymptomatic) multiple myeloma: IMWG consensus perspectives risk factors for progression and guidelines for monitoring and management. *Leukemia.* 2010;24(6):1121-1127.
3. De Smedt E, Lui H, Maes K, et al. The Epigenome in Multiple Myeloma: Impact on Tumor Cell Plasticity and Drug Response. *Frontiers in oncology.* 2018;8:566.
4. Casciello F, Windloch K, Gannon F, Lee JS. Functional Role of G9a Histone Methyltransferase in Cancer. *Frontiers in immunology.* 2015;6:487.
5. Barski A, Cuddapah S, Cui K, et al. High-resolution profiling of histone methylations in the human genome. *Cell.* 2007;129(4):823-837.
6. Tu WB, Shiah YJ, Lourenco C, et al. MYC Interacts with the G9a Histone Methyltransferase to Drive Transcriptional Repression and Tumorigenesis. *Cancer cell.* 2018;34(4):579-595 e578.
7. Tachibana M, Matsumura Y, Fukuda M, Kimura H, Shinkai Y. G9a/GLP complexes independently mediate H3K9 and DNA methylation to silence transcription. *EMBO J.* 2008;27(20):2681-2690.
8. Zhang XY, Rajagopalan D, Chung TH, et al. Frequent upregulation of G9a promotes RelB-dependent proliferation and survival in multiple myeloma. *Exp Hematol Oncol.* 2020;9:8.
9. Guan X, Zhong X, Men W, Gong S, Zhang L, Han Y. Analysis of EHMT1 expression and its correlations with clinical significance in esophageal squamous cell cancer. *Molecular and clinical oncology.* 2014;2(1):76-80.
10. Segovia C, San Jose-Eneriz E, Munera-Maravilla E, et al. Inhibition of a G9a/DNMT network triggers immune-mediated bladder cancer regression. *Nature medicine.* 2019;25(7):1073-1081.
11. San Jose-Eneriz E, Agirre X, Rabal O, et al. Discovery of first-in-class reversible dual small molecule inhibitors against G9a and DNMTs in hematological malignancies. *Nature communications.* 2017;8:15424.
12. Dupere-Richer D, Licht JD. Epigenetic regulatory mutations and epigenetic therapy for multiple myeloma. *Curr Opin Hematol.* 2017;24(4):336-344.
13. Moreaux J, Klein B, Bataille R, et al. A high-risk signature for patients with multiple myeloma established from the molecular classification of human myeloma cell lines. *Haematologica.* 2011;96(4):574-582.
14. Maes K, Boeckx B, Vlummens P, et al. The genetic landscape of 5T models for multiple myeloma. *Scientific reports.* 2018;8(1):15030.
15. Goyvaerts C, De Vlaeminck Y, Escors D, et al. Antigen-presenting cell-targeted lentiviral vectors do not support the development of productive T-cell effector responses: implications for in vivo targeted vaccine delivery. *Gene Ther.* 2017;24(6):370-375.
16. Mulligan G, Mitsiades C, Bryant B, et al. Gene expression profiling and correlation with outcome in clinical trials of the proteasome inhibitor bortezomib. *Blood.* 2007;109(8):3177-3188.
17. Herviou L, Kassambara A, Boireau S, et al. PRC2 targeting is a therapeutic strategy for EZ score defined high-risk multiple myeloma patients and overcome resistance to IMiDs. *Clin Epigenetics.* 2018;10(1):121.
18. Gentleman RC, Carey VJ, Bates DM, et al. Bioconductor: open software development for computational biology and bioinformatics. *Genome biology.* 2004;5(10):R80.
19. Kassambara A, Reme T, Jourdan M, et al. GenomicScape: an easy-to-use web tool for gene expression data analysis. Application to investigate the molecular events in the differentiation of B cells into plasma cells. *PLoS Comput Biol.* 2015;11(1):e1004077.

20. Kassambara A, Hose D, Moreaux J, et al. Genes with a spike expression are clustered in chromosome (sub)bands and spike (sub)bands have a powerful prognostic value in patients with multiple myeloma. *Haematologica.* 2012;97(4):622-630.
21. Hothorn T, Zeileis A. Generalized maximally selected statistics. *Biometrics.* 2008;64(4):1263-1269.
22. Kocaturk NM, Akkoc Y, Kig C, Bayraktar O, Gozuacik D, Kutlu O. Autophagy as a molecular target for cancer treatment. *Eur J Pharm Sci.* 2019;134:116-137.
23. Ntanasis-Stathopoulos I, Fotiou D, Terpos E. CCL3 Signaling in the Tumor Microenvironment. *Advances in experimental medicine and biology.* 2020;1231:13-21.
24. Hatakeyama S. TRIM Family Proteins: Roles in Autophagy, Immunity, and Carcinogenesis. *Trends Biochem Sci.* 2017;42(4):297-311.
25. Li Y, Li N, Yan Z, et al. Dysregulation of the NLRP3 inflammasome complex and related cytokines in patients with multiple myeloma. *Hematology.* 2016;21(3):144-151.
26. Wake NC, Ricketts CJ, Morris MR, et al. UBE2QL1 is disrupted by a constitutional translocation associated with renal tumor predisposition and is a novel candidate renal tumor suppressor gene. *Hum Mutat.* 2013;34(12):1650-1661.
27. Wang T, Tao W, Zhang L, Li S. Oncogenic role of microRNA-20a in human multiple myeloma. *Onco Targets Ther.* 2017;10:4465-4474.
28. Cao H, Li L, Yang D, et al. Recent progress in histone methyltransferase (G9a) inhibitors as anticancer agents. *Eur J Med Chem.* 2019;179:537-546.
29. Artal-Martinez de Narvajas A, Gomez TS, Zhang JS, et al. Epigenetic regulation of autophagy by the methyltransferase G9a. *Molecular and cellular biology.* 2013;33(20):3983-3993.
30. Ding J, Li T, Wang X, et al. The histone H3 methyltransferase G9A epigenetically activates the serine-glycine synthesis pathway to sustain cancer cell survival and proliferation. *Cell metabolism.* 2013;18(6):896-907.
31. Kim Y, Kim YS, Kim DE, et al. BIX-01294 induces autophagy-associated cell death via EHMT2/G9a dysfunction and intracellular reactive oxygen species production. *Autophagy.* 2013;9(12):2126-2139.
32. Acevo-Rodriguez PS, Maldonado G, Castro-Obregon S, Hernandez G. Autophagy Regulation by the Translation Machinery and Its Implications in Cancer. *Frontiers in oncology.* 2020;10:322.
33. Pierzynowska K, Gaffke L, Cyske Z, et al. Autophagy stimulation as a promising approach in treatment of neurodegenerative diseases. *Metab Brain Dis.* 2018;33(4):989-1008.
34. Bhutia SK, Mukhopadhyay S, Sinha N, et al. Autophagy: cancer's friend or foe? *Advances in cancer research.* 2013;118:61-95.
35. Ahmad F, Dixit D, Joshi SD, Sen E. G9a inhibition induced PKM2 regulates autophagic responses. *The international journal of biochemistry & cell biology.* 2016;78:87-95.
36. Li F, Zeng J, Gao Y, et al. G9a Inhibition Induces Autophagic Cell Death via AMPK/mTOR Pathway in Bladder Transitional Cell Carcinoma. *PloS one.* 2015;10(9):e0138390.
37. Yin C, Ke X, Zhang R, et al. G9a promotes cell proliferation and suppresses autophagy in gastric cancer by directly activating mTOR. *FASEB journal : official publication of the Federation of American Societies for Experimental Biology.* 2019;33(12):14036-14050.
38. Tong J, Yu Q, Xu W, et al. Montelukast enhances cytocidal effects of carfilzomib in multiple myeloma by inhibiting mTOR pathway. *Cancer biology & therapy.* 2019;20(3):381-390.
39. Eichner R, Fernandez-Saiz V, Targosz BS, Bassermann F. Cross Talk Networks of Mammalian Target of Rapamycin Signaling With the Ubiquitin Proteasome System and Their Clinical Implications in Multiple Myeloma. *Int Rev Cell Mol Biol.* 2019;343:219-297.
40. Farrell AS, Sears RC. MYC degradation. *Cold Spring Harb Perspect Med.* 2014;4(3).
41. Miller DM, Thomas SD, Islam A, Muench D, Sedoris K. c-Myc and cancer metabolism. *Clinical cancer research : an official journal of the American Association for Cancer Research.* 2012;18(20):5546-5553.

42. Holien T, Misund K, Olsen OE, et al. MYC amplifications in myeloma cell lines: correlation with MYC-inhibitor efficacy. *Oncotarget.* 2015;6(26):22698-22705.
43. Moller HEH, Preiss BS, Pedersen P, et al. Myc protein overexpression is a feature of progression and adverse prognosis in multiple myeloma. *European journal of haematology.* 2018.
44. Liu P, Ge M, Hu J, et al. A functional mammalian target of rapamycin complex 1 signaling is indispensable for c-Myc-driven hepatocarcinogenesis. *Hepatology.* 2017;66(1):167-181.
45. Shin JM, Jeong YJ, Cho HJ, Magae J, Bae YS, Chang YC. Suppression of c-Myc induces apoptosis via an AMPK/mTOR-dependent pathway by 4-O-methyl-ascochlorin in leukemia cells. *Apoptosis.* 2016;21(5):657-668.
46. Poole CJ, van Riggelen J. MYC-Master Regulator of the Cancer Epigenome and Transcriptome. *Genes (Basel).* 2017;8(5).
47. Carew JS, Espitia CM, Zhao W, et al. Rational cotargeting of HDAC6 and BET proteins yields synergistic antimyeloma activity. *Blood advances.* 2019;3(8):1318-1329.
48. Delmore JE, Issa GC, Lemieux ME, et al. BET bromodomain inhibition as a therapeutic strategy to target c-Myc. *Cell.* 2011;146(6):904-917.
49. Shi J, Vakoc CR. The mechanisms behind the therapeutic activity of BET bromodomain inhibition. *Molecular cell.* 2014;54(5):728-736.
50. Bruyer A, Maes K, Herviou L, et al. DNMTi/HDACi combined epigenetic targeted treatment induces reprogramming of myeloma cells in the direction of normal plasma cells. *British journal of cancer.* 2018.
51. Shaffer AL, Emre NC, Lamy L, et al. IRF4 addiction in multiple myeloma. *Nature.* 2008;454(7201):226-231.
52. Sakamaki JI, Wilkinson S, Hahn M, et al. Bromodomain Protein BRD4 Is a Transcriptional Repressor of Autophagy and Lysosomal Function. *Molecular cell.* 2017;66(4):517-532 e519.
53. Rhyasen GW, Hattersley MM, Yao Y, et al. AZD5153: A Novel Bivalent BET Bromodomain Inhibitor Highly Active against Hematologic Malignancies. *Molecular cancer therapeutics.* 2016;15(11):2563-2574.
54. Lub S, Maes K, Menu E, De Bruyne E, Vanderkerken K, Van Valckenborgh E. Novel strategies to target the ubiquitin proteasome system in multiple myeloma. *Oncotarget.* 2016;7(6):6521-6537.
55. Ghobrial IM, Weller E, Vij R, et al. Weekly bortezomib in combination with temsirolimus in relapsed or relapsed and refractory multiple myeloma: a multicentre, phase 1/2, open-label, dose-escalation study. *The lancet oncology.* 2011;12(3):263-272.
56. Deng C, Lipstein MR, Scotto L, et al. Silencing c-Myc translation as a therapeutic strategy through targeting PI3Kdelta and CK1epsilon in hematological malignancies. *Blood.* 2017;129(1):88-99.
57. Yao R, Sun X, Xie Y, et al. Identification of a novel c-Myc inhibitor with antitumor effects on multiple myeloma cells. *Biosci Rep.* 2018;38(5).
58. Zhao R, Chen M, Jiang Z, et al. Platycodin-D Induced Autophagy in Non-Small Cell Lung Cancer Cells via PI3K/Akt/mTOR and MAPK Signaling Pathways. *J Cancer.* 2015;6(7):623-631.
59. Chen L, Wang S, Zhou Y, et al. Identification of early growth response protein 1 (EGR-1) as a novel target for JUN-induced apoptosis in multiple myeloma. *Blood.* 2010;115(1):61-70.

9. Figure legends

Figure 1: Prognostic value and expression of G9a and GLP in MM. A) The expression profile of G9a and GLP was investigated in the MMRF cohort (n=674). **B-D)** The prognostic value of G9a in terms of overall survival (OS) was determined in newly diagnosed MM patients using the MMRF (B, n=674) and the Montpellier cohort (C, n=68) and in relapsed MM patients from the Mulligan cohort (D, n=188). Maxstat analysis was used to calculate the optimal separation of patients based on a cutoff value.

Figure 2: Effect of G9a/GLP-targeting on MM cell viability, proliferation and apoptosis. A) Effect of UNC0638 or BIX01294 on cell viability. Cells were treated with increasing doses of UNC0638 and BIX01294. After 4 days, cell viability was assessed using the CellTiter-Glo Luminescent Cell viability assay. Data represent the IC50 value (in µM) calculated based on at least 3 independent experiments. **B-C)** Effect of UNC0638 or BIX01294 on proliferation. OPM-2 and XG-20 cells were treated with indicated concentrations of UNC0638 or BIX01294 for 48h and 72h. Using flow cytometry, cell cycle profiles based on DNA content were obtained after 72h (B) and Ki67 levels after 48h (C). Data represents mean ± SD of 3 independent experiments. **D)** Effect of UNC0638 or BIX01294 on apoptosis. OPM-2, XG-7 and XG-20 cells were treated with indicated doses of UNC0638 or BIX01294 for 48h. The effect on apoptosis was assessed using an annexinV-APC/7'AAD staining followed by flow cytometric analysis. The % apoptotic cells are the sum of the percentage annexinV (+) and annexinV (+)/7'AAD (+) cells. Data represent the mean ± SD of 3 independent experiments. * indicates $p<0.05$ compared to control. **E)** Effect of BIX01294 on primary human CD138+ MM cells. Mononuclear cells from 12 MM patients were treated with increasing doses of BIX01294 and cultured in the presence of IL-6 (1ng/mL). At day 4, the percentage CD138+ viable plasma cells was determined by flow cytometry. Bars represent values relative to control.

Figure 3: Effect of inducible knockdown of G9a. A-B) Validation of G9a knockdown. XG-7 cells were transduced with 3 different shG9a constructs and cultured with or without doxycycline (Dox, 1 mg/ml) for 3 or 5 days after which G9a mRNA (A) and protein (B) levels were analyzed using qRT-PCR and western blot respectively. For the qRT-PCR data, data represent the mean ± SD of 3 independent experiments. For the western blot data, tubulin

was used as loading control and one experiment representative of 3 is shown. **C)** Effect of G9a knockdown on cumulative cell growth. XG-7 cells transduced with shG9a construct 1 (shG9a#1) were cultured with or without doxycycline (Dox, 1 mg/ml) for 14 days. Cumulative cell counts were measured using trypan blue staining on indicated time points. Results shown are the mean ± SD of 4 independent experiments. * indicates $p<0.05$ compared to control (CTR).

Figure 4: Underlying mechanisms of action of G9a/GLP-targeting in MM. **A-B)** Effect of G9a/GLP-targeting on H3K9me1-3 levels. A) Western blot analysis of H3K9me1, H3K9me2 and H3K9me3 levels in OPM-2 and XG-7 cells after 96h of treatment with or without BIX01294 (2 µM). B) XG-7 cells transduced with 3 different shG9a constructs were cultured with or without doxycycline (Dox, 1 mg/ml) for 7 days after which H3K9me2 and H3K9me3 levels were analyzed by western blot. Histone 3 was used as loading control and one experiment representative of 3 is shown. Quantification and normalization was performed with Image J and quantification relative to the control condition is shown. **C)** Effect of G9a/GLP-targeting on autophagy. Immunofluorescence staining for DAPI, LC3B and α-tubulin on OPM-2 and XG-20 cells treated with or without 5µM BIX01294 or UNC0638 for 24h. Scale bar = 10 µm. Pictures shown are representative of 1 experiment, quantification data are based on 3 independent experiments. *** indicates $p<0.005$, **** indicates $p<0.001$. **D-E)** Western blot analysis of involved signaling pathways and downstream targets. OPM-2 (D) and XG-7 (E) cells were treated with 1,25 µM, 2,5µM and 5µM BIX01294 for 24h after which whole cell lysates were analyzed for indicated proteins. Tubulin was used as loading control and one experiment representative of 3 is shown. **F)** mRNA expression levels of MYC and eIF4E in OPM-2 and XG-7 cells treated with or without 5µM BIX01294 for 24h. Data represents mean ± SD of 3 independent experiments. * indicates $p<0.05$. **G)** Effect of the autophagy inhibitor 3-methyladenine on BIX01294 induced cell death. OPM-2 cells were pre-treated for 4 hours with 3-methyladenine (1 & 2 mM) after which BIX01294 (2,5 µM) was added for an additional 48 hours. The effect on apoptosis was assessed using an annexinV-APC/7'AAD staining followed by flow cytometric analysis. The % apoptotic cells are the sum of the percentage annexinV (+) and annexinV (+)/7'AAD (+) cells. Data represent the mean ± SD of 3 independent experiments. * indicates $p<0.05$ compared to treatment with BIX01294 alone.

Figure 5: Association of G9a/GLP-targeting and epigenetic repressive marks. A) Molecular signature of G9a/GLPi-target genes in three HMCLs (OPM-2, XG20 and XG24) was investigated using GSEA Database (all curated gene sets) and relevant pathways are presented (FDR q value ≤ 0.05). **B)** mRNA expression levels of CCL3 in OPM-2 and XG-7 cells treated with or without 5µM BIX01294 for 24h. Data represents mean ± SD of 3 independent experiments. * indicates p<0.05. **C)** Integrative genomics viewer (IGV) visualization of H3K9me3 enrichment on EGR2, TRIM69, UB2QL1, and CASP1 genes in XG-7 cells.

Figure 6: Effect of BIX01294 treatment on tumor progression in the murine 5TGM1 model. A-B) Effect of G9a/GLP-targeting on murine MM cell viability (A) and apoptosis (B). A) The murine MM cell lines 5T33vv, 5T33vt and 5TGM1 were treated with increasing doses of UNC0638 and BIX01294. After 4 days, cell viability was assessed using CellTiter-Glo Luminescent Cell viability assay. Data represent the IC50 value (in µM) calculated based on at least 3 independent experiments. B) Effect of BIX01294 on apoptosis. 5T33vt and 5TGM1 cells were treated with indicated doses BIX01294 for 48h. The effect on apoptosis was assessed using an annexinV-APC/7'AAD staining followed by flow cytometric analysis. The % apoptotic cells are the sum of the percentage annexinV (+) and annexinV (+)/7'AAD (+) cells. Data represent the mean ± SD of 3 independent experiments. **C-E)** Effect of G9a/GLP-targeting on tumor burden (D) and overall survival (E) in the murine 5TGM1 model. C) Scheme depicting the experimental setup. Mice were inoculated with 5TGM1 cells and treated for 14 days with vehicle (n=11) or 10 mg/kg BIX (n=11, 3 times a week). Treatment started 14 days after tumor inoculation. D) Tumor burden was monitored at day 30 by bioluminescent imaging (BLI) measuring total photon flux. BLI images from 3 mice from each treatment group are shown. E) Effect of BIX01294 on overall survival. Difference in overall survival was assayed with a log-rank test and survival curves plotted using the Kaplan-Meier method. * indicates p<0.05.

Figure 7: Effect of BIX01294 on MM cell sensitivity towards proteasome inhibitors. A-C) Effect of G9a/GLP-targeting on carfilzomib induced cell death. A) Effect of carfilzomib and/or BIX01294 treatment on human cell lines. Human OPM-2 and XG-7 cells were treated with indicated concentrations of carfilzomib (Cfz) and/or BIX01294 (BIX) for 4 days. The viability was determined by using the CellTiter-Glo assay and synergy scores were calculated

using the Bliss method. Results are the mean of 3 independent experiments. B) Effect of G9a knockdown on carfilzomib induced cell death. Transduced XG-7 shG9a#1 cells were cultured with increasing doses of carfilzomib 3 days after treatment with or without doxycycline (Dox) for an additional 4 days. The viability was determined using the CellTiter-Glo assay. Results shown are the mean ± SD of 4 independent experiments. * indicates $p<0.05$, ** indicates $p<0.005$, *** indicates $p<0.001$. C) Effect of carfilzomib and/or BIX01294 treatment on primary human CD138+ MM cells. Mononuclear cells from 7 MM patients were treated with indicated concentrations for 4 days and the percentage CD138+ viable plasma cells was determined by flow cytometry. Results are expressed as the relative viability compared to control. **D)** Western blot analysis of the mechanisms underlying the increased carfilzomib sensitivity upon BIX01294 treatment. XG-7 cells were treated with BIX01294 (2µM) and/or 2nM carfilzomib (2nM) for 24h, after which western blot analysis was performed on whole cell lysates for indicated proteins. Actin was used as loading control and one experiment representative of 3 is shown. **E-F)** Effect of BIX01294 (BIX) and bortezomib (Bz) combination treatment on tumor burden (E) and survival (F) in the murine 5TGM1 model. Mice were inoculated with 5TGM1 cells and assigned to different treatment groups receiving either vehicle, 10 mg/kg BIX, 0.6 mg/kg Bz or a combination of both. The number of mice per treatment group and the treatment scheme is indicated in the schematic overview (upper). To determine the effect on tumor burden (E), all mice were sacrificed when the first mouse showed clear signs of morbidity. * indicates $p<0.05$, *** indicates $p<0.001$. To determine the effect on overall survival (F), each mouse was sacrificed individually when showing clear signs of morbidity and the effect on survival rates was determined by Kaplan-Meier analysis. * indicates $p<0.05$ compared to treatment with Bz alone.

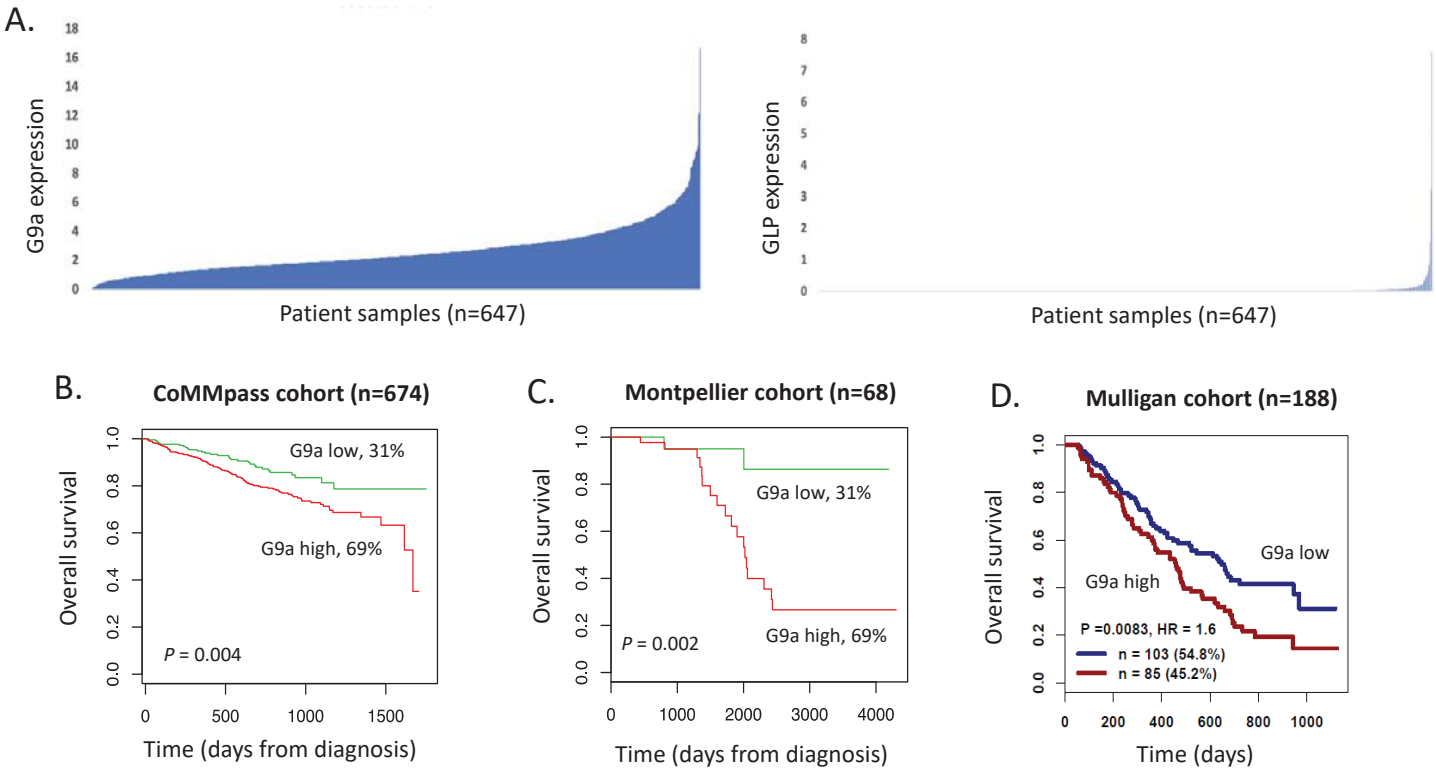
A.
G9a expression
Patient samples (n=647)
GLP expression
Patient samples (n=647)
B.
CoMMpass cohort (n=674)
G9a low, 31%
G9a high, 69%
P = 0.004
Overall survival
Time (days from diagnosis)
C.
Montpellier cohort (n=68)
G9a low, 31%
G9a high, 69%
P = 0.002
Overall survival
Time (days from diagnosis)
D.
Mulligan cohort (n=188)
G9a low
G9a high
P =0.0083, HR = 1.6
n = 103 (54.8%)
n = 85 (45.2%)
Overall survival
Time (days)

Figure 1

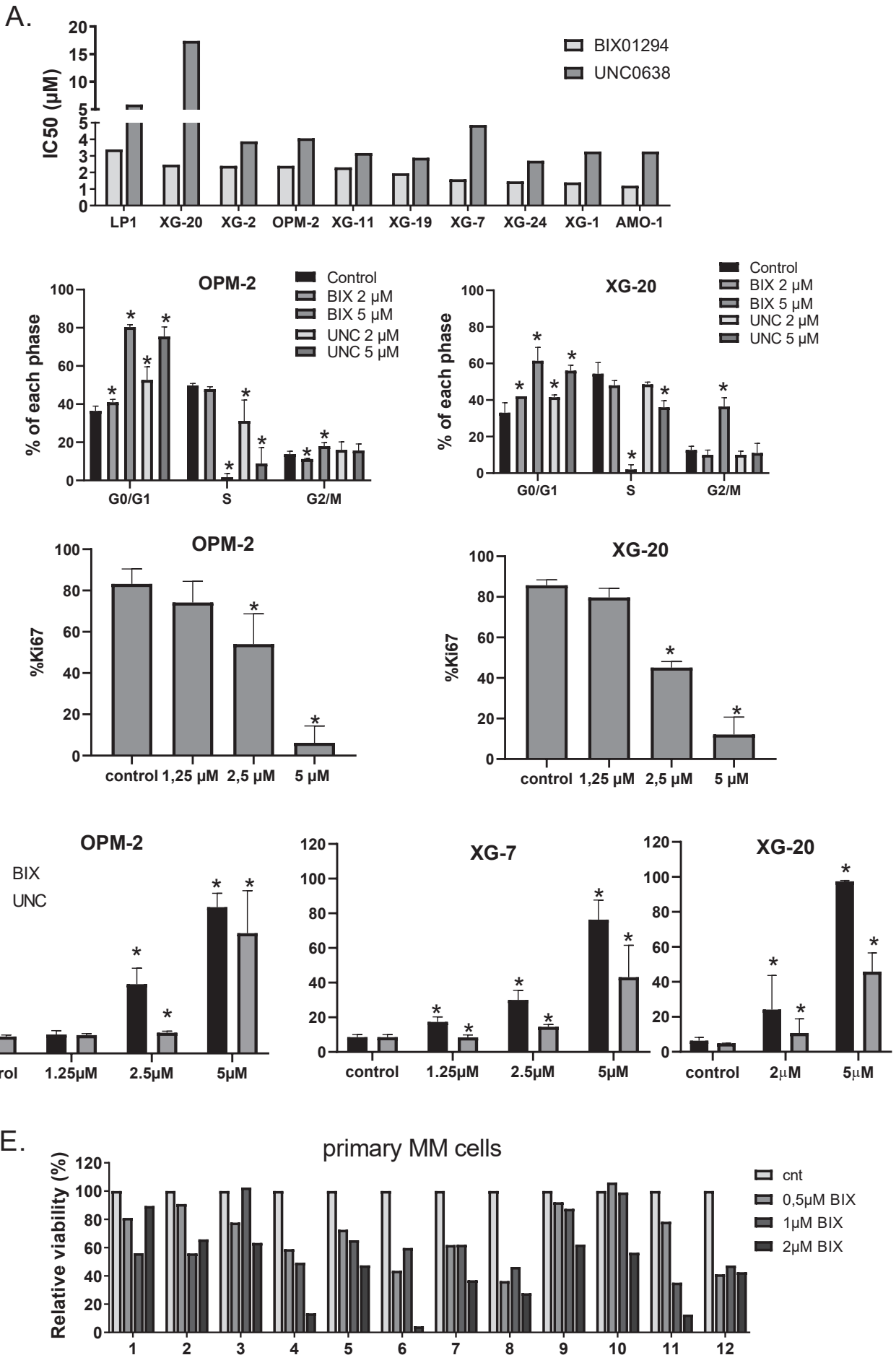
A.
IC50 (μM)
BIX01294
UNC0638
LP1
XG-20
XG-2
OPM-2
XG-11
XG-19
XG-7
XG-24
XG-1
AMO-1
B.
OPM-2
XG-20
% of each phase
Control
BIX 2 μM
BIX 5 μM
UNC 2 μM
UNC 5 μM
G0/G1
S
G2/M
C.
OPM-2
XG-20
%Ki67
control
1,25 μM
2,5 μM
5 μM
D.
OPM-2
XG-7
XG-20
% apoptotic cells
BIX
UNC
control
1.25μM
2.5μM
5μM
2μM
E.
primary MM cells
Relative viability (%)
cnt
0,5μM BIX
1μM BIX
2μM BIX

A.

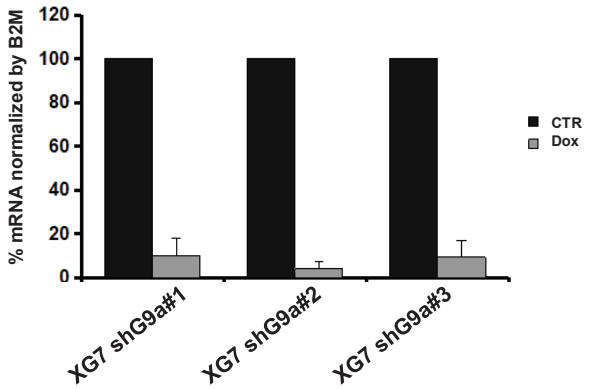
% mRNA normalized by B2M
120
100
80
60
40
20
0
CTR
Dox
XG7 shG9a#1
XG7 shG9a#2
XG7 shG9a#3

B.

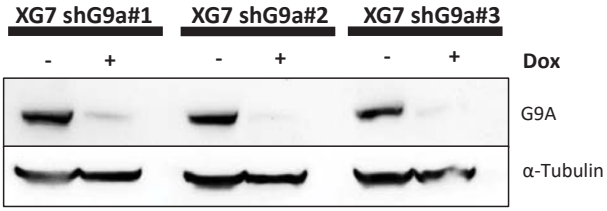
XG7 shG9a#1
XG7 shG9a#2
XG7 shG9a#3
- + - + - +
Dox
G9A
α-Tubulin

C.

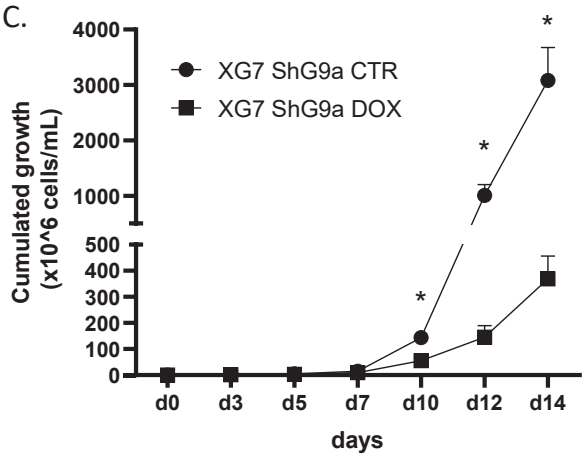
Cumulated growth
(x10^6 cells/mL)
4000
3000
2000
1000
500
400
300
200
100
0
XG7 ShG9a CTR
XG7 ShG9a DOX
*
*
*
d0
d3
d5
d7
d10
d12
d14
days

Figure 3

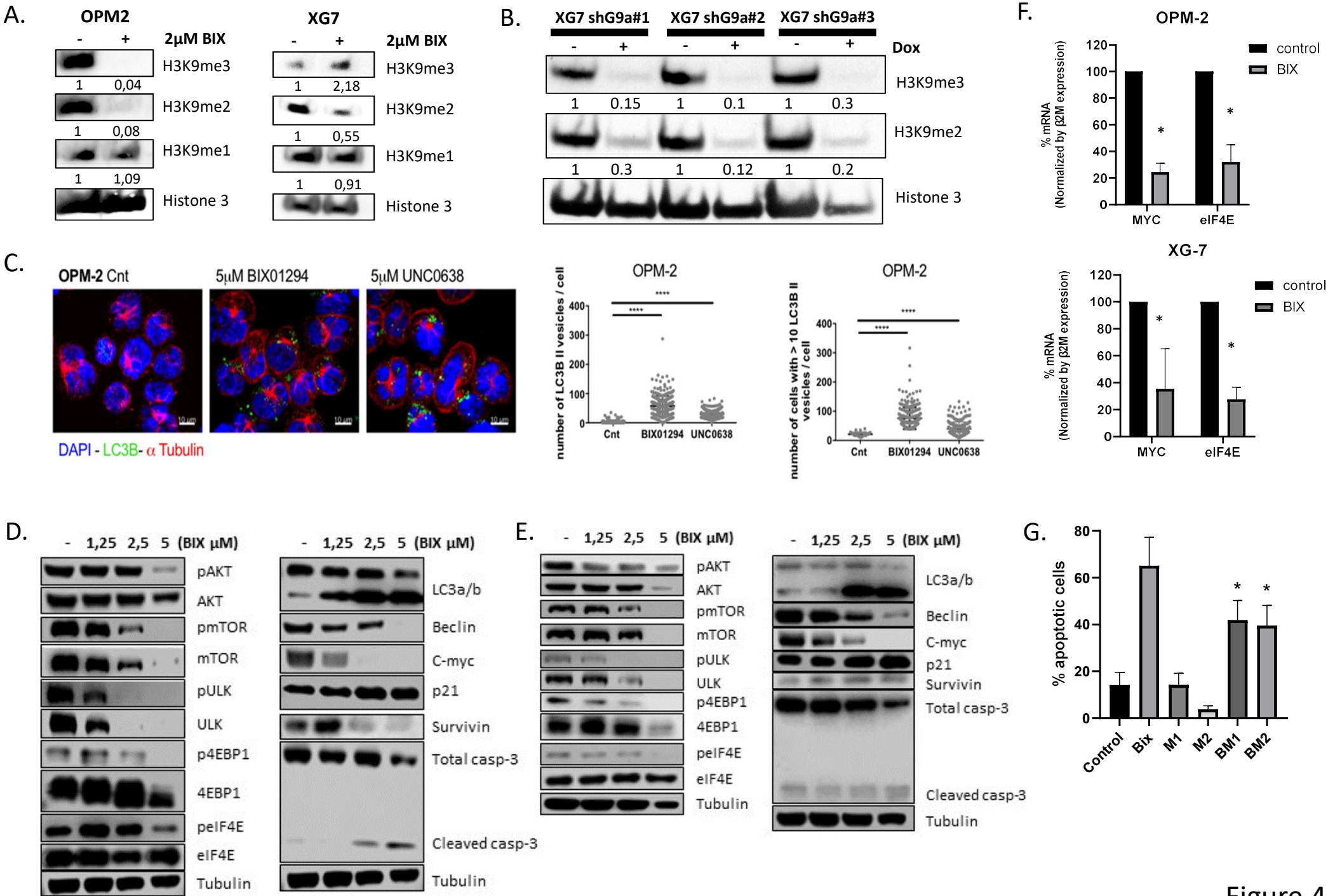
A.
OPM2
XG7
2μM BIX
H3K9me3
H3K9me2
H3K9me1
Histone 3
1 0,04
1 0,08
1 1,09
1 2,18
1 0,55
1 0,91
B.
XG7 shG9a#1
XG7 shG9a#2
XG7 shG9a#3
Dox
1 0.15 1 0.1 1 0.3
1 0.3 1 0.12 1 0.2
C.
OPM-2 Cnt
5μM BIX01294
5μM UNC0638
DAPI - LC3B- α Tubulin
number of LC3B II vesicles / cell
number of cells with > 10 LC3B II vesicles / cell
Cnt
BIX01294
UNC0638
F.
OPM-2
XG-7
control
BIX
% mRNA (Normalized by β2M expression)
MYC
eIF4E
D.
- 1,25 2,5 5 (BIX μM)
pAKT
AKT
pmTOR
mTOR
pULK
ULK
p4EBP1
4EBP1
peIF4E
eIF4E
Tubulin
LC3a/b
Beclin
C-myc
p21
Survivin
Total casp-3
Cleaved casp-3
E.
G.
% apoptotic cells
Control
Bix
M1
M2
BM1
BM2

Figure 4

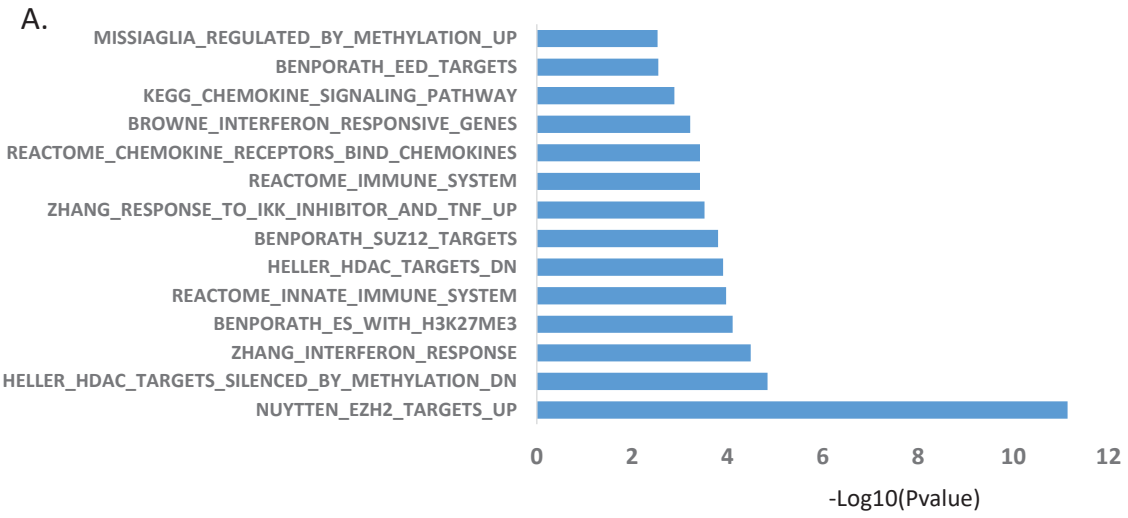
A.
MISSIAGLIA_REGULATED_BY_METHYLATION_UP
BENPORATH_EED_TARGETS
KEGG_CHEMOKINE_SIGNALING_PATHWAY
BROWNE_INTERFERON_RESPONSIVE_GENES
REACTOME_CHEMOKINE_RECEPTORS_BIND_CHEMOKINES
REACTOME_IMMUNE_SYSTEM
ZHANG_RESPONSE_TO_IKK_INHIBITOR_AND_TNF_UP
BENPORATH_SUZ12_TARGETS
HELLER_HDAC_TARGETS_DN
REACTOME_INNATE_IMMUNE_SYSTEM
BENPORATH_ES_WITH_H3K27ME3
ZHANG_INTERFERON_RESPONSE
HELLER_HDAC_TARGETS_SILENCED_BY_METHYLATION_DN
NUYTTEN_EZH2_TARGETS_UP
0
2
4
6
8
10
12
-Log10(Pvalue)

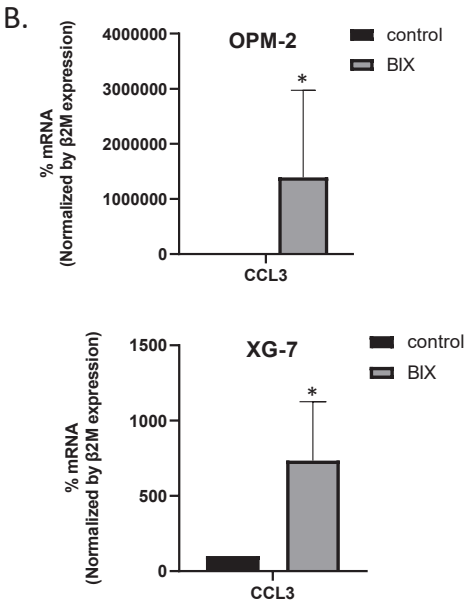
B.
OPM-2
control
BIX
% mRNA (Normalized by β2M expression)
4000000
3000000
2000000
1000000
0
CCL3
XG-7
control
BIX
% mRNA (Normalized by β2M expression)
1500
1000
500
0
CCL3

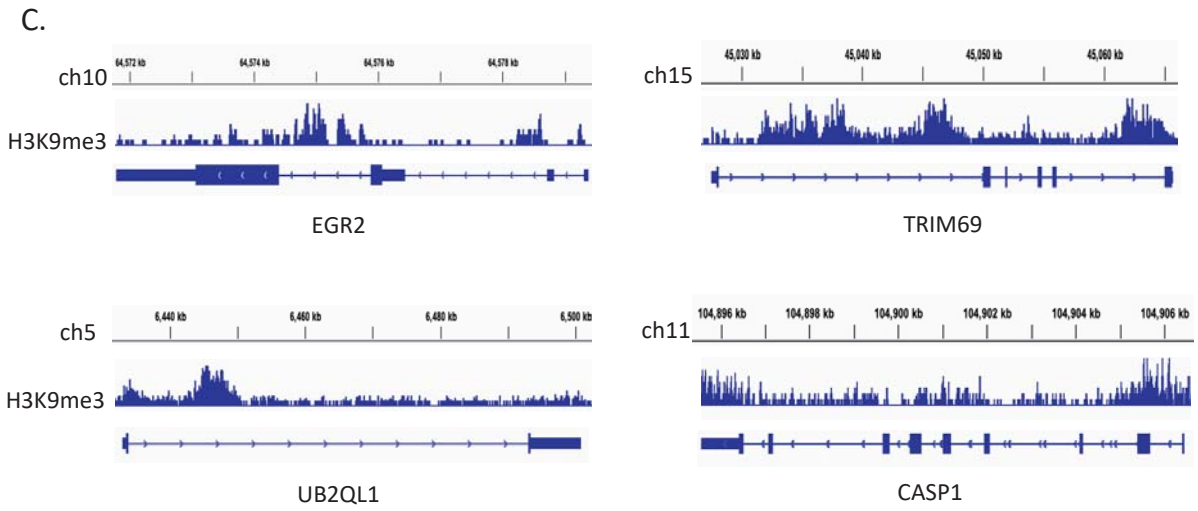
C.
ch10
H3K9me3
EGR2
ch15
TRIM69
ch5
H3K9me3
UB2QL1
ch11
CASP1

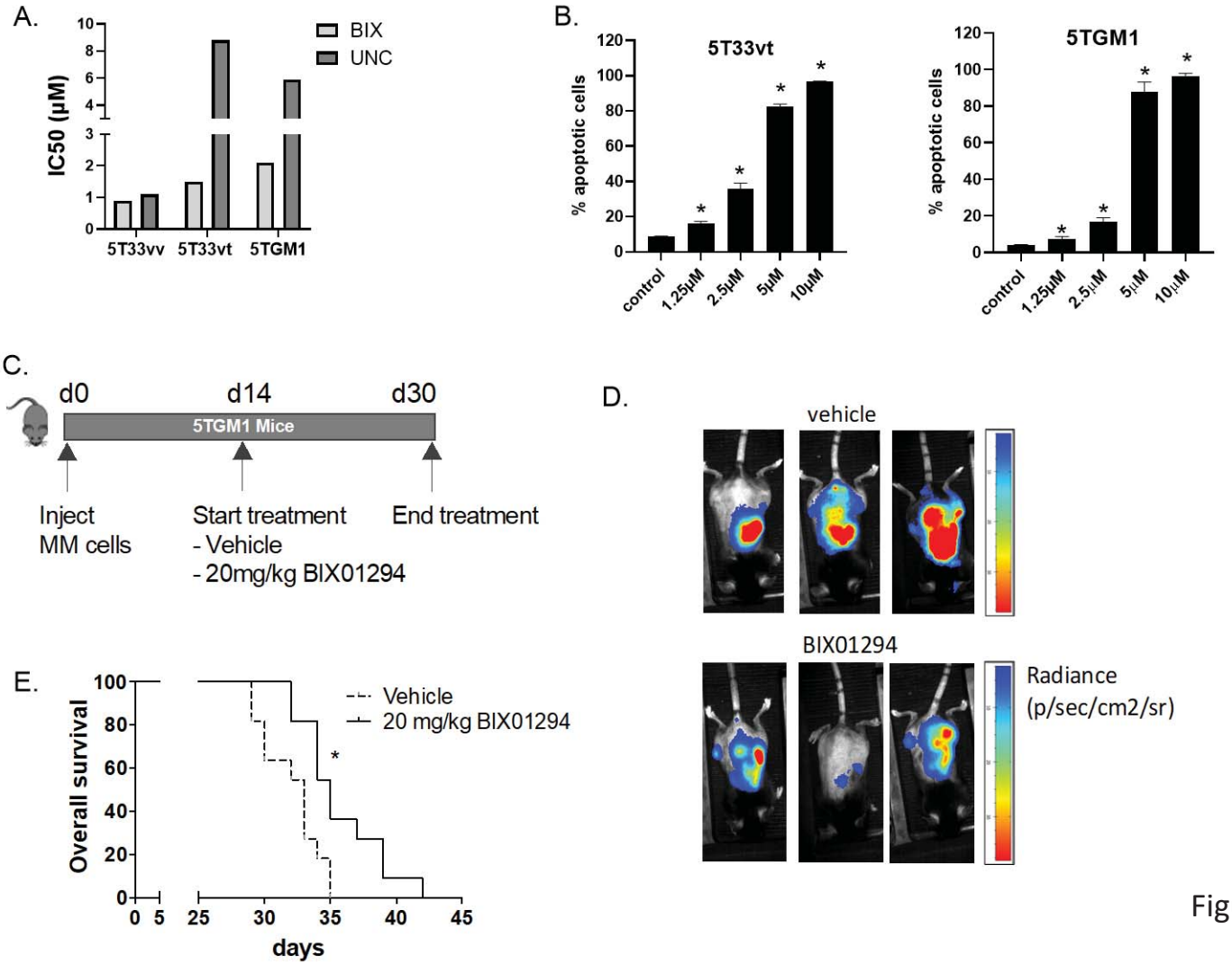
A.
IC50 (μM)
BIX
UNC
5T33vv
5T33vt
5TGM1
B.
5T33vt
% apoptotic cells
control
1.25μM
2.5μM
5μM
10μM
5TGM1
C.
d0
d14
d30
5TGM1 Mice
Inject
MM cells
Start treatment
- Vehicle
- 20mg/kg BIX01294
End treatment
D.
vehicle
BIX01294
Radiance
(p/sec/cm2/sr)
E.
Overall survival
Vehicle
20 mg/kg BIX01294
days

Figure 6

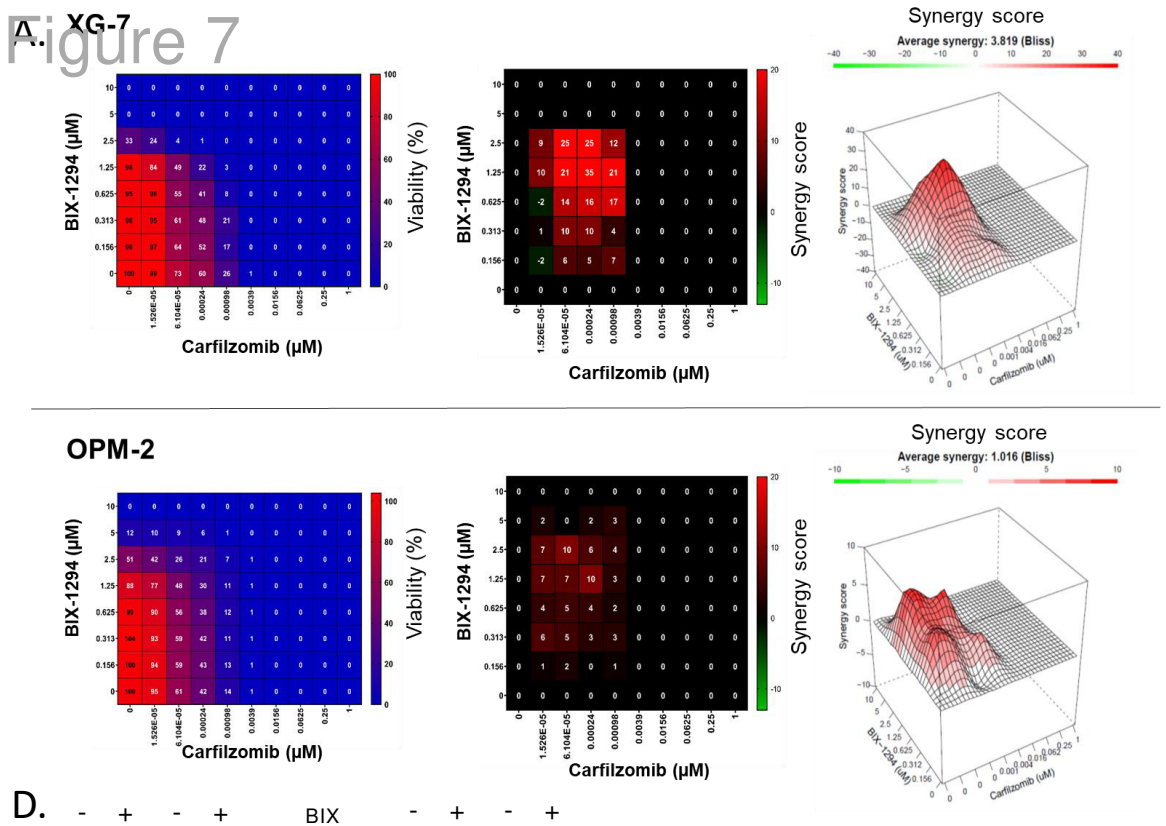
A.
XG-7
BIX-1294 (μM)
Carfilzomib (μM)
Viability (%)
Synergy score
Average synergy: 3.819 (Bliss)
OPM-2
Average synergy: 1.016 (Bliss)

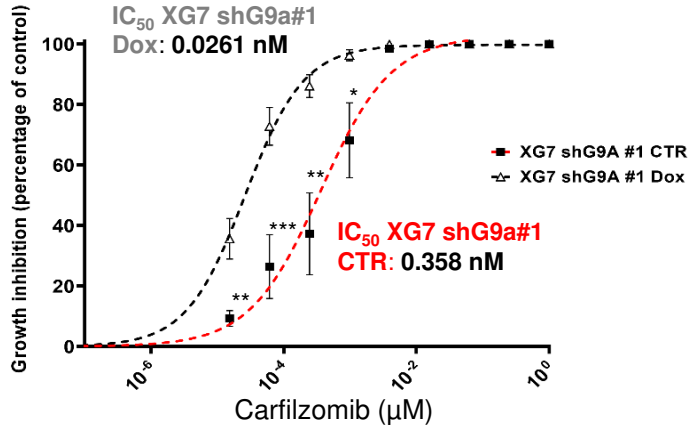
B.
IC50 XG7 shG9a#1
Dox: 0.0261 nM
XG7 shG9A #1 CTR
XG7 shG9A #1 Dox
IC50 XG7 shG9a#1
CTR: 0.358 nM
Growth inhibition (percentage of control)
Carfilzomib (μM)

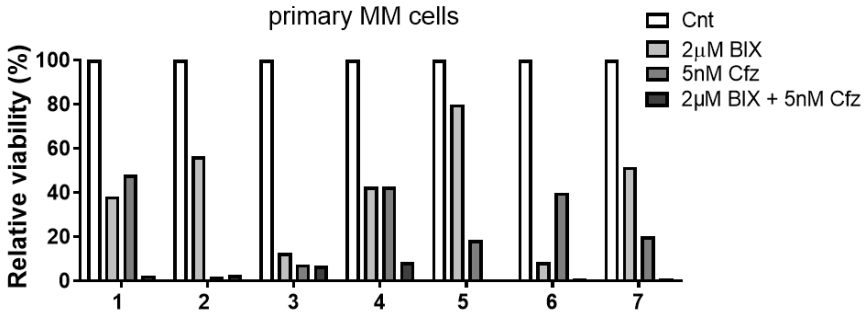
C.
primary MM cells
Cnt
2μM BIX
5nM Cfz
2μM BIX + 5nM Cfz
Relative viability (%)

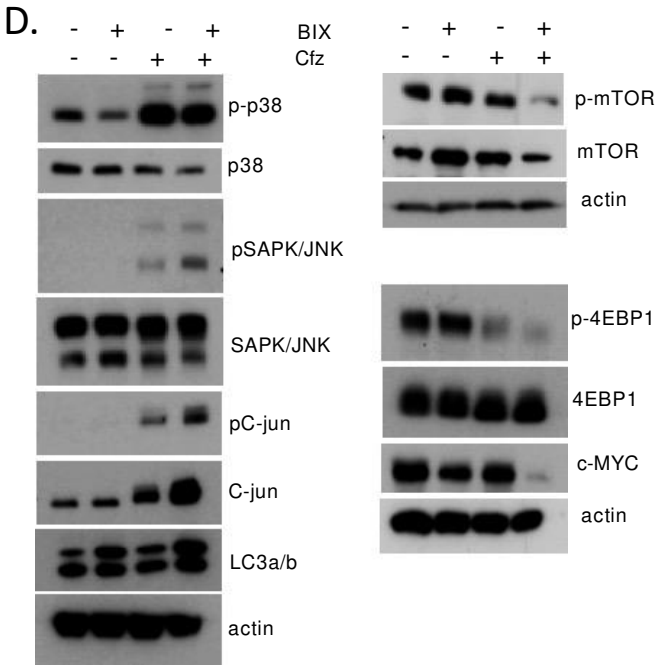
D.
BIX
Cfz
p-p38
p38
pSAPK/JNK
SAPK/JNK
pC-jun
C-jun
LC3a/b
actin
p-mTOR
mTOR
actin
p-4EBP1
4EBP1
c-MYC
actin

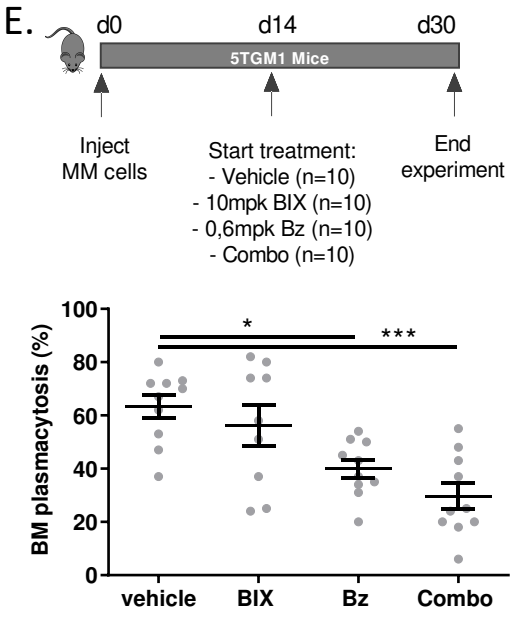
E.
d0
d14
d30
5TGM1 Mice
Inject MM cells
Start treatment:
- Vehicle (n=10)
- 10mpk BIX (n=10)
- 0,6mpk Bz (n=10)
- Combo (n=10)
End experiment
BM plasmacytosis (%)
vehicle
BIX
Bz
Combo

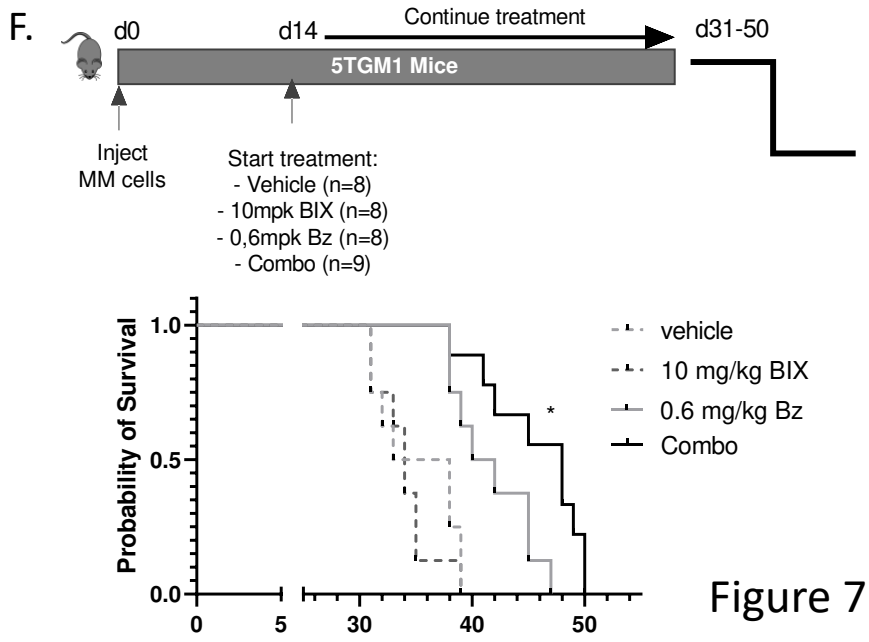
F.
d0
d14
Continue treatment
d31-50
5TGM1 Mice
Inject MM cells
Start treatment:
- Vehicle (n=8)
- 10mpk BIX (n=8)
- 0,6mpk Bz (n=8)
- Combo (n=9)
Probability of Survival
vehicle
10 mg/kg BIX
0.6 mg/kg Bz
Combo

Figure 7